

Disulfide Bonding among μ 1 Trimers in Mammalian Reovirus Outer Capsid: a Late and Reversible Step in Virion Morphogenesis

Amy L. Odegard,^{1,2} Kartik Chandran,¹ Susanne Liemann,³ Stephen C. Harrison,⁴
and Max L. Nibert^{1*}

*Departments of Microbiology and Molecular Genetics¹ and Biological Chemistry and Molecular Pharmacology,⁴
Harvard Medical School, and Laboratory of Molecular Medicine and Howard Hughes Medical Institute,
Children's Hospital,³ Boston, Massachusetts 02115, and Department of Biochemistry, University
of Wisconsin—Madison, Madison, Wisconsin 53706²*

Received 15 October 2002/Accepted 5 February 2003

We examined how a particular type of intermolecular disulfide (ds) bond is formed in the capsid of a cytoplasmically replicating nonenveloped animal virus despite the normally reducing environment inside cells. The μ 1 protein, a major component of the mammalian reovirus outer capsid, has been implicated in penetration of the cellular membrane barrier during cell entry. A recent crystal structure determination supports past evidence that the basal oligomer of μ 1 is a trimer and that 200 of these trimers surround the core in the fenestrated T=13 outer capsid of virions. We found in this study that the predominant forms of μ 1 seen in gels after the nonreducing disruption of virions are ds-linked dimers. Cys679, near the carboxyl terminus of μ 1, was shown to form this ds bond with the Cys679 residue from another μ 1 subunit. The crystal structure in combination with a cryomicroscopy-derived electron density map of virions indicates that the two subunits that contribute a Cys679 residue to each ds bond must be from adjacent μ 1 trimers in the outer capsid, explaining the trimer-dimer paradox. Successful *in vitro* assembly of the outer capsid by a nonbonding mutant of μ 1 (Cys679 substituted by serine) confirmed the role of Cys679 and suggested that the ds bonds are not required for assembly. A correlation between μ 1-associated ds bond formation and cell death in experiments in which virions were purified from cells at different times postinfection indicated that the ds bonds form late in infection, after virions are exposed to more oxidizing conditions than those in healthy cells. The infectivity measurements of the virions with differing levels of ds-bonded μ 1 showed that these bonds are not required for infection in culture. The ds bonds in purified virions were susceptible to reduction and reformation *in situ*, consistent with their initial formation late in morphogenesis and suggesting that they may undergo reduction during the entry of reovirus particles into new cells.

The manner in which disulfide (ds) bonds are formed in proteins is a matter of continued interest (1, 26, 37, 52, 55). The extracellular proteins of both prokaryotes and eukaryotes are rich in ds bonds, but intracellular proteins are not (however, see reference 37 regarding archaeal microbes). In fact, ds bonds are rarely found in intracellular proteins aside from those involved in reduction-oxidation (redox) reactions. The chemically reducing environment inside cells is the primary determinant of the rarity of stable intracellular ds bonds in proteins. As for many other cellular phenomena, studies of ds bond formation in viruses have contributed to our present understanding and have identified instructive variations and exceptions.

Intra- and intermolecular ds bonds, formed within the oxidizing environment of the endoplasmic reticulum (ER), are common in the surface proteins of enveloped animal viruses (6, 54). The ds bonds generally contribute to the folding and stability of these proteins. An ER-localized enzyme, protein ds isomerase, is critical for forming most of these bonds. Vaccinia virus, an enveloped virus that assembles its membrane-bound particles in the reducing environment of the cytoplasm, en-

codes its own thiol oxidoreductases (E10R, A2.5L, and G4L), which mediate the formation of ds bonds in at least two viral membrane proteins (55, 56, 65). Since these three enzymes are required for the morphogenesis of vaccinia virions, formation of these ds bonds is likely essential.

Although the capsid proteins of most nonenveloped animal viruses also fold within the reducing cytoplasmic environment, ds bonds have been identified in a number of them as well. Intermolecular ds bonds link subunits of the major capsid proteins of papovaviruses and are proposed to play roles in their assembly, stability, and disassembly (22, 31, 33, 53). It is not yet clear when and how these bonds are formed, but recent evidence for simian virus 40 suggests that capsid molecules with intramolecular ds bonds are transitory intermediates in the pathway (32). Intra- or intermolecular ds bonds have been identified in the capsids of some picornaviruses (28, 35) and parvoviruses (62), but their roles are poorly understood. In adenovirus virions, the viral proteinase is ds linked to its 11-residue cofactor, pVIc, which may keep the two from dissociating at low concentrations (40). In rotaviruses, which use an atypical mechanism for outer capsid assembly involving the budding of particles into the ER lumen with subsequent loss of the budded membrane, intramolecular ds bonds are found in the outer capsid proteins VP4 and VP7 (44, 48). In VP7, these ds bonds are critical for its folding in the ER and assembly into

* Corresponding author. Mailing address: Department of Microbiology and Molecular Genetics, Harvard Medical School, 200 Longwood Ave., Boston, MA 02115. Phone: (617) 645-3680. Fax: (617) 738-7664. E-mail: mnibert@hms.harvard.edu.

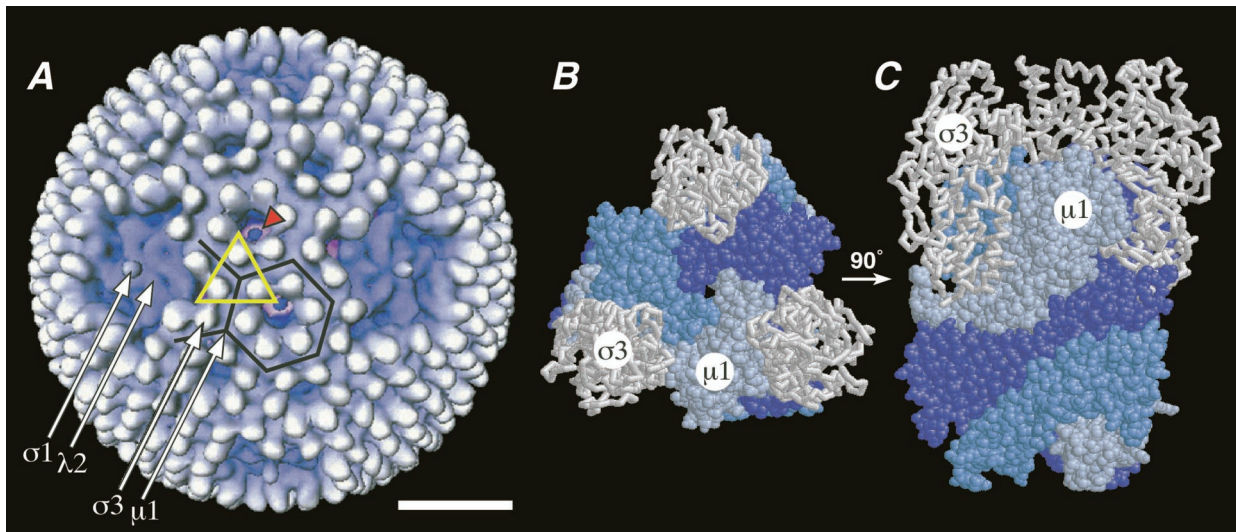


FIG. 1. Reovirus outer capsid and $\mu 1$. (A) Surface view of the virion from cryoEM and 3D image reconstruction (16). Features attributable to outer capsid proteins $\sigma 1$, $\lambda 2$, $\sigma 3$, and $\mu 1$ are visible and marked by arrows. The particle display was radially depth cued to enhance the recognition of symmetrical features (59). One $\mu 1$ - $\sigma 3$ heterohexamamer, shown in crystallographic detail in panels B and C (34), is enclosed in an open yellow triangle. Six subunits of $\sigma 3$, associated with six different $\mu 1$ - $\sigma 3$ heterohexamers, surround each P3 channel, one of which is enclosed in a black hexagon. A blob of density is visible within each of these channels (red arrowhead; see Discussion for more information) (15, 16). Four subunits of $\sigma 3$, associated with four different $\mu 1$ - $\sigma 3$ heterohexamers, surround each P2 channel, one of which is enclosed in a black partial hexagon. Bar, 20 nm. (B and C) Top and side views, respectively, of the $\mu 1$ - $\sigma 3$ heterohexamamer by X-ray crystallography (34). The heterohexamamer is shown in the same orientation from the top as the one enclosed by the triangle in panel A (note the three white $\sigma 3$ subunits at the triangle's corners). The $\sigma 3$ and $\mu 1$ subunits are shown in backbone and space-filling formats, respectively. The three interwound subunits of $\mu 1$ within its trimer are shown in different shades of blue.

particles and are probably formed with the aid of protein disomerase.

Nonfusogenic mammalian orthoreoviruses (reoviruses) form 85-nm virions (Fig. 1A) that contain the segmented double-stranded RNA genome enclosed by two concentric icosahedral protein capsids. The inner capsid includes the machinery for RNA synthesis, and the outer capsid includes that for entry into the host cytoplasm, where reovirus replication and assembly occur (reviewed in reference 46). Outer capsid protein $\sigma 1$ (50 kDa, 36 copies) forms fiber-like trimers that extend from the fivefold axes of virions and bind to cellular receptors (3, 4, 10, 18, 30, 60). Outer capsid protein $\mu 1$ (76 kDa, 600 copies), which appears in virions mostly as the autolytically cleaved fragments $\mu 1N$ (4 kDa) and $\mu 1C$ (72 kDa), is thought to mediate viral penetration of the cellular membrane barrier during entry (7, 8, 19, 20, 34, 36, 45, 47). A subvirion particle (partial disassembly intermediate) containing a protease-sensitive, lipophilic conformer of $\mu 1$ appears to be involved in this activity (7). Outer capsid protein $\sigma 3$ (41 kDa, 600 copies), the major surface protein of virions, interacts closely with $\mu 1$ and limits its conformational lability until removed by proteolysis during entry (16, 23, 34, 43). Outer capsid protein $\lambda 2$ (144 kDa, 60 copies) forms pentameric turrets that surround the fivefold axes and bridge the inner and outer capsids (16, 51, 64). It is involved in the 5' capping and release of the viral mRNA molecules (11, 16, 17, 38, 51). The viral genome, the inner capsid proteins, and $\lambda 2$ constitute a transcriptionally active subvirion particle called the core that is both an intermediate in virion assembly and the product of partial disassembly that accompanies entry (reviewed in reference 46).

Smith et al. (58) reported, but did not show supporting

evidence, that if reovirus virions are dissociated without reducing agent, the $\mu 1C$ protein band is absent from a subsequent gel and an increased amount of material is seen near the λ proteins, which are about twice the M_r of $\mu 1C$. They concluded that $\mu 1C$ either is a ds-bonded dimer in virions or associates to form such dimers when virions are disrupted under nonreducing conditions. A later study from the same laboratory provided evidence for slowly sedimenting species of $\mu 1C$ and $\sigma 3$ in glycerol gradients, consistent with the existence of the ds-linked dimers of $\mu 1C$ in solution (21). We believe, however, that those slowly sedimenting species were more likely the 350-kDa $\mu 1$ - $\sigma 3$ heterohexamers for which a crystal structure was recently determined (34) (Fig. 1). These heterohexamers are the precursors for assembly of the fenestrated T=13 lattice of $\mu 1$ - $\sigma 3$ that surrounds the viral core and constitutes most of the virion outer capsid (8, 16, 34, 42, 57) (Fig. 1). No other demonstrations of ds-bonded dimers of $\mu 1/\mu 1C$ have appeared in the literature since these early reports. Moreover, the more recent structural evidence that a trimer is the basal oligomer of $\mu 1$ (16, 34) raises questions about the presence and locations of the ds bonds. Given the reducing environment in healthy cells, the cytoplasmic assembly of reovirus virions also raises questions about when and how these bonds may form.

In the present study, we demonstrated that the ds-bonded dimers of $\mu 1$ are present in reovirus virions and that each ds bond is formed by the Cys679 residues from two $\mu 1$ subunits. We also showed that these bonds form late in virion morphogenesis, in dead or dying cells; that they are not required for assembly of the outer capsid, the basic stability of virions, or particle infectivity; and that they can be reversibly reduced and reformed within intact virions. The locations of the ds bonds

within the outer capsid, based on a fit of the crystallographic model of the μ 1- σ 3 heterohexamer into a cryomicroscopy-derived electron density map of virions (34), indicates that each ds bond is formed between subunits from adjacent μ 1 trimers. As many as 300 of these bonds in total thus cross-link the 200 μ 1 trimers across the particle surface. These results explain how a particular type of intermolecular ds bond is formed in the capsid of a cytoplasmically replicating nonenveloped animal virus despite the normally reducing environment inside cells.

MATERIALS AND METHODS

Cells. Spinner-adapted murine L929 cells for the production of reovirus stocks and purified virions were grown in Joklik's modified minimal essential medium (Irvine Scientific) supplemented to contain 2% fetal bovine serum and 2% bovine calf serum (HyClone Laboratories), 2 mM glutamine, 100 U of penicillin/ml, and 100 μ g of streptomycin (Irvine Scientific)/ml. *Spodoptera frugiperda* clone 21 and *Trichoplusia ni* High Five insect cells (Invitrogen) were grown in TC-100 medium (Gibco BRL) supplemented to contain 10% heat-inactivated fetal bovine serum and were used, respectively, for preparing baculovirus stocks and expressing the reovirus μ 1 and σ 3 proteins from baculovirus vectors for reconstituting cores. *S. frugiperda* clone 21 cells were alternatively grown in Hink's TNM-FH insect medium (JRH Biosciences) supplemented to contain 10% fetal bovine serum (Sigma) and were used in preparing baculovirus stocks and in expressing the μ 1 and σ 3 proteins from baculovirus vectors for purifying the μ 1- σ 3 complexes.

Purified virions. Unless otherwise indicated, virions of reovirus type 1 Lang (T1L), type 2 Jones, and type 3 Dearing (T3D) were purified by the standard protocol involving freon extraction and CsCl gradient centrifugation (45) and were stored in virion storage buffer (10 mM Tris-HCl [pH 7.5], 150 mM NaCl, 10 mM $MgCl_2$) at 4°C prior to use. Iodoacetamide at a concentration of 50 mM (IAM; Sigma) was added during the course of some purifications as indicated in the legend to Fig. 6. Particle concentrations were determined from the A_{260} (13, 58). Infectious titers of the purified virion preparations were determined with a standard, protease-free plaque assay as described previously (18). For making [^{35}S]methionine-cysteine- and [3H]myristate-labeled virions, previously described protocols for metabolic labeling were used (45, 47). Purified infectious subvirion particles (ISVPs) of reovirus T1L were obtained as previously described (45) except that the durations of treatment were 20 min with chymotrypsin and either 5 or 30 min with trypsin.

SDS-PAGE. Several types of gel sample buffer were used in these studies. In the earliest experiments, standard reducing Laemmli buffer (62.5 mM Tris-HCl [pH 6.8], 10% glycerol, 2% sodium dodecyl sulfate (SDS), 5% β -mercaptoethanol [BME], 0.004% bromophenol blue) was used (29). In subsequent experiments, based on initial findings and other considerations, several changes were introduced. To improve buffering capacity, the concentration of Tris was increased; for ease of preparation, sucrose was substituted for glycerol; to improve the resolution of protein bands in the gels, the concentrations of SDS and BME were reduced; and to aid in the gel-loading process, the concentration of bromophenol blue was increased. As a result, for all but the earliest experiments, the standard reducing sample buffer included 125 mM Tris-HCl, 10% sucrose, 1% SDS, 2% BME, and 0.01% bromophenol blue. In addition, because of the poor buffering capacity of Tris at pH 6.8 and the lower reactivity of most sulfhydryl groups at that pH, pH 8.0 sample buffer was adopted as the standard for most experiments (see Fig. 3 for supporting evidence). Dithiothreitol (DTT; 5 mM) was substituted for BME as the reducing agent in some experiments as indicated in the legends to Fig. 3B, 5, and 7. For the complementary nonreducing sample buffers, reducing agent was omitted and 50 mM IAM was added as a sulfhydryl-blocking agent unless otherwise indicated (see legend to Fig. 2). When IAM was used, a 20- to 30-min incubation at room temperature was included before loading the samples on the gel to allow this reagent to react with free cysteine residues. Protein disruption was accomplished by incubation for 2 min in a boiling water bath unless otherwise indicated. Single-percentage and gradient polyacrylamide gel electrophoresis (PAGE) gels in full- and mini-sized formats were used as indicated in the figure legends. Visualization of protein bands by staining and fluorography was performed as previously described (45).

Partial proteolytic analysis of protein gel bands. Purified [^{35}S]methionine-cysteine-labeled virions of reovirus T3D were disrupted for 5 min at 60°C in reducing (5% BME) or nonreducing (50 mM IAM) sample buffer (pH 6.8) and subjected to SDS-PAGE (10% acrylamide). After electrophoresis, protein bands

were visualized by staining with Coomassie brilliant blue R-250 for 30 min and destaining for 60 min at 4°C. The μ 1C band from the lanes of reduced samples and the major high- M_r band from the lanes of nonreduced samples were excised from the gel. These gel pieces were separately incubated in reducing soaking buffer (pH 6.8 sample buffer with 0.1% SDS and 5% BME) for 30 min at room temperature to resolve any ds-bonded species. The gel pieces were next incubated for 30 min at room temperature in nonreducing soaking buffer (0% BME) to remove the reducing agent and loaded into wells atop a discontinuous SDS-PAGE (5 to 20% acrylamide) gradient gel. The gel pieces were overlaid with nonreducing sample buffer (0% BME, pH 6.8) that included differing amounts of *N* α -*p*-tosyl-L-lysine chloromethyl ketone (TLCK)-treated bovine α -chymotrypsin (Sigma). The samples were subjected to electrophoresis until the dye front had moved halfway through the stacking gel, at which time electrophoresis was stopped for 30 min to allow chymotrypsin digestion of the stacked proteins. Electrophoresis was resumed until the dye front reached the bottom of the resolving gel, and the gel was prepared for fluorography.

Protease digestions of native virions. Purified virions of reovirus T1L or T3D at a concentration of 1×10^{12} or 2×10^{12} particles/ml were treated with 100 μ g of *N*-tosyl-L-phenylalanine chloromethyl ketone (TPCK)-treated bovine trypsin (Sigma)/ml for different times at 32°C in virion storage buffer. At each time point, a sample was removed to 4°C and adjusted to contain 300 μ g of soybean trypsin inhibitor/ml to terminate digestion. Samples were mixed with reducing and/or nonreducing sample buffer for analysis by SDS-PAGE. Experiments with TLCK-treated bovine α -chymotrypsin were performed in an identical manner except that the protease was used at 200 μ g/ml and inhibited at the end of each reaction by removing the sample to 4°C and adding phenylmethylsulfonyl fluoride to a concentration of 2 mM.

Analysis of excised gel bands in a second gel. Purified trypsin-generated ISVPs (30-min trypsin treatment to obtain the putative ϕ : ϕ dimer band and 5-min trypsin treatment to obtain the putative μ 1C: ϕ dimer band) were disrupted in nonreducing sample buffer and subjected to SDS-PAGE in the duplicate lanes of a mini-sized gel (1.5-mm thickness; 15 and 8% acrylamide for ϕ : ϕ and μ 1C: ϕ , respectively). The gel was stained with Coomassie brilliant blue R-250 for 5 min and destained until the bands were clearly visible at room temperature (about 5 min), after which the bands were excised. One gel slice was incubated in reducing soaking buffer (pH 8.0 sample buffer with 0.1% SDS and 1% BME), while the other was incubated in nonreducing soaking buffer (0% BME) for 30 min at room temperature. Each gel slice was then diced and carefully loaded into the dry wells of a second mini-sized gel (1.5-mm thickness; 15 and 13% acrylamide for ϕ : ϕ and μ 1C: ϕ , respectively). The gel slices were overlaid with reducing (1% BME) or nonreducing (50 mM IAM) sample buffer (pH 8.0). After markers were loaded into adjacent wells, the gels were subjected to electrophoresis and staining as usual.

Recombinant baculoviruses. A recombinant baculovirus for expressing the reovirus T1L μ 1 (from the T1L M2 gene) and σ 3 (from the T1L S4 gene) proteins in insect cells was described previously (17). To make a recombinant baculovirus for expressing a mutant μ 1 in which a serine residue was substituted for Cys679 (C679S), the first step involved site-directed mutagenesis of the template plasmid pBKS-M2L (8) by using the QuikChange protocol (Stratagene). The complementary mutagenic primers 5'-CGCACITTC~~CC~~GGCGCTAAGCCCCACTCTCCGACCAACGG-3' and 5'-CCGTTGGTCGGAGAGTCGGGCTTAGGCGCGGAAAGTTCGG-3' (underlining indicates changes from the wild type [wt]) were used to introduce the desired nucleotide changes. Clones containing these changes were identified by loss of the *Hae*I restriction site. The mutant clones were sequenced between the *Age*I and *Hind*III restriction sites (nucleotides 1876 to 2225 of T1L M2) to confirm that only the desired nucleotide changes had been introduced in that region. The *Age*I-*Hind*III fragment was then subcloned into the transposition plasmid pFbD-M2L-S4L (17), which was used to generate a recombinant baculovirus with the Bac-to-Bac system (Gibco BRL) as previously described (8).

Purified μ 1- σ 3 complexes. Heterohexamer complexes of the reovirus T1L μ 1 and σ 3 proteins, formed after the infection of *S. frugiperda* clone 21 cells with a μ 1- σ 3 dual-expressing recombinant baculovirus (8), were purified as described previously (34). μ 1- σ 3 complexes containing the μ 1 mutant C679S were expressed and purified by using the same protocol. For IAM modification, the proteins were first reduced by incubation at 37°C for 30 min in Tris-HCl (pH 8.5) with 10 mM DTT. The DTT was removed with a PD-10 column (Amersham Pharmacia Biotech), and the buffer was replaced with 20 mM Tris-HCl (pH 8.0)-100 mM NaCl-2 mM $MgCl_2$. IAM was then added to 10 mM and incubated for 30 min at room temperature in the dark. Excess IAM was removed with a PD-10 column. For storage, the protein was shock-frozen in liquid N_2 and stored at -80°C. The storage buffer for all preparations contained 20 mM Bicine-HCl (pH 9.0), 100 mM NaCl, 2 mM $MgCl_2$, 10 mM DTT, and 0.02% NaN_3 .

Electrospray ionization ion trap mass spectrometry was performed by David King at the Howard Hughes Medical Institute, University of California at Berkeley. Prior to mass spectrometry, 10- μ g aliquots of each protein sample were desalted by micropore reversed-phase high-performance liquid chromatography (Michrom UMA) with a Polymer Labs RP300 column and a 20 to 60% gradient of acetonitrile in 0.1% trifluoroacetic acid in water. The identity and purity of the eluted proteins were assessed directly by flow injection at 1 μ l/min into the electrospray ion source of a Bruker-Agilent Esquire ion trap mass spectrometer.

Recoated cores. Purified cores of reovirus T1L were obtained as previously described (8). Cores were recoated with μ 1- σ 3 complexes (with or without the C679S mutation in μ 1) from lysates of *T. ni* High Five cells by using the previously described protocol (8). Recoated cores containing C679S- μ 1 exhibited indistinguishable behavior on the CsCl gradients used to purify them as recoated cores containing wt μ 1. The concentrations of particles in the purified preparations were determined by densitometric quantitations of the λ band intensities from SDS-PAGE gels after using different amounts of purified T1L virions to generate a standard curve.

Molecular graphics. The arrangements of six μ 1 trimers around a P3 channel and four μ 1 trimers around a P2 channel were obtained by a three-dimensional (3D) fit of the crystallographic μ 1- σ 3 model into an electron density map of the virion obtained by transmission electron cryomicroscopy (cryoEM) and 3D image reconstruction as previously described (34). The crystallographic model of a λ 2 pentamer from the core (51) was also fit into the same map for depiction of the P2 channel. After fitting, the electron density map and crystallographic models of all σ 3 subunits were removed from both depictions. The crystal structure images in Fig. 1 and 8 were created, respectively, with RasMac version 2.7.1 and with Molscript and Raster3D (27, 41), and the final versions of both figures were assembled in Illustrator version 8.0 (Adobe Systems).

Determination of cell viability. Trypan blue staining was used as a measure of cell viability over time courses of infection for the purification of virions. Immediately before the harvesting cells from an infected spinner culture, a 50- μ l aliquot of the suspension was removed and mixed with 450 μ l of 0.4% trypan blue solution (Sigma). The sample was dispensed onto a hemacytometer, and the cells were scored as dead/dying (stained) or living (not stained) by viewing them with an inverted phase microscope. At least 450 cells were scored from each culture.

Reversibility of ds bond formation in virions. The time course of ds bond reduction was carried out at room temperature by adding DTT (5 mM final concentration) to purified T1L virions in pH 8.0 buffer (150 mM NaCl, 50 mM Tris-HCl). The reaction was quenched at each time point by adding IAM (50 mM final concentration). The time course of ds bond reoxidation was performed by first reducing the ds bonds in purified T1L virions by exposing them to 5 mM DTT for 30 min at room temperature in the pH 8.0 buffer described above. The DTT was removed by dialysis into pH 8.0 buffer for 3 h at room temperature. Cystine (Sigma) was then added (5 mM final concentration) to promote ds bond formation. Samples were incubated at room temperature and quenched with IAM (50 mM final concentration) at each time point. For each time course, nonreducing sample buffer was added prior to disruption for electrophoresis.

RESULTS

SDS-PAGE of nonreduced μ 1C from virions suggests it forms ds-bonded dimers. We disrupted the purified virions of reovirus T3D in sample buffers containing decreasing concentrations of BME as reducing agent and resolved the proteins by SDS-PAGE. At 1% BME, the standard protein profile was seen (Fig. 2, lane 1), but at lower concentrations, a new high- M_r band, migrating closely above the λ band, appeared (Fig. 2, lanes 4 to 6). In parallel, the major μ 1C band decreased in intensity (Fig. 2, lanes 4 to 6). The M_r of the new band was about 155,000, consistent with that for a ds-bonded dimer of the 72-kDa μ 1C protein. After reduction with BME, protein from the excised high- M_r band comigrated in a second SDS-PAGE gel with monomeric μ 1C ($M_r \approx 75,000$) (data not shown). Essentially identical results with decreasing concentrations of BME were obtained with the purified virions of reoviruses T1L (data not shown, but see Fig. 3) and type 2 Jones (data not shown). This indicates that the apparent ds

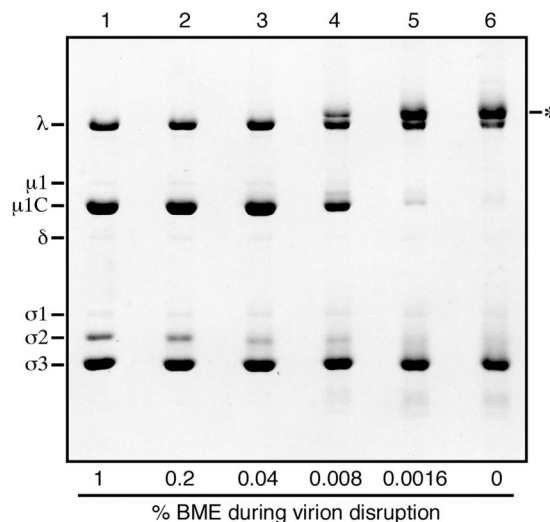


FIG. 2. Effects of reduced concentrations of BME on the migration of reovirus proteins during SDS-PAGE. Purified virions of reovirus T3D were mixed with pH 6.8 sample buffers containing decreasing concentrations of BME and disrupted in a boiling water bath. The viral proteins were then resolved on a full-sized SDS-PAGE (10% acrylamide) gel and visualized by Coomassie staining. Known positions of the viral proteins are indicated by name. The major new high- M_r band observed at low BME concentrations is also indicated (*).

bonding of μ 1C in virions is conserved among members of the three reovirus serotypes. When DTT was used as the reducing agent, the high- M_r form of μ 1C became evident in SDS-PAGE gels when virions were disrupted at DTT concentrations below 0.8 mM.

In the preceding experiments, some downward smearing of other viral protein bands was seen when BME or DTT was reduced in concentration or omitted. This was most notable for the σ 2 and σ 3 proteins (Fig. 2, lanes 3 to 6). Evidence in the next section suggests this smearing reflects the formation of intramolecular ds bonds within these proteins after the disruption of virions.

Effects of a sulfhydryl-blocking agent on the appearance of ds-bonded μ 1C. To determine whether the ds-bonded form of μ 1C is present before the disruption of virions, we used the sulfhydryl-blocking agent IAM to modify free cysteine residues in μ 1C. T1L virions were disrupted by heating in the absence of reducing agent, and IAM (50 mM) was added before electrophoresis. IAM had no effect on the disappearance of the μ 1C band and appearance of the new high- M_r band (Fig. 3A, lanes 2 to 4). In a following experiment, the addition of IAM before virion disruption also showed no effect on the disappearance of the μ 1C band and appearance of the new high- M_r band (Fig. 3B, lanes 2 and 4). These results provide evidence that the ds-bonded form of μ 1C is formed in virions before disruption (see below for further evidence). Chymotrypsin digests (12) of the excised high- M_r band obtained after virion disruption in the presence of IAM again identified μ 1C as the predominant component of this band (Fig. 3C). Essentially the same results with IAM were obtained with the purified virions of reovirus T3D (data not shown).

Addition of IAM decreased the smearing of other viral protein bands (e.g., that of σ 2 and σ 3) and also decreased the

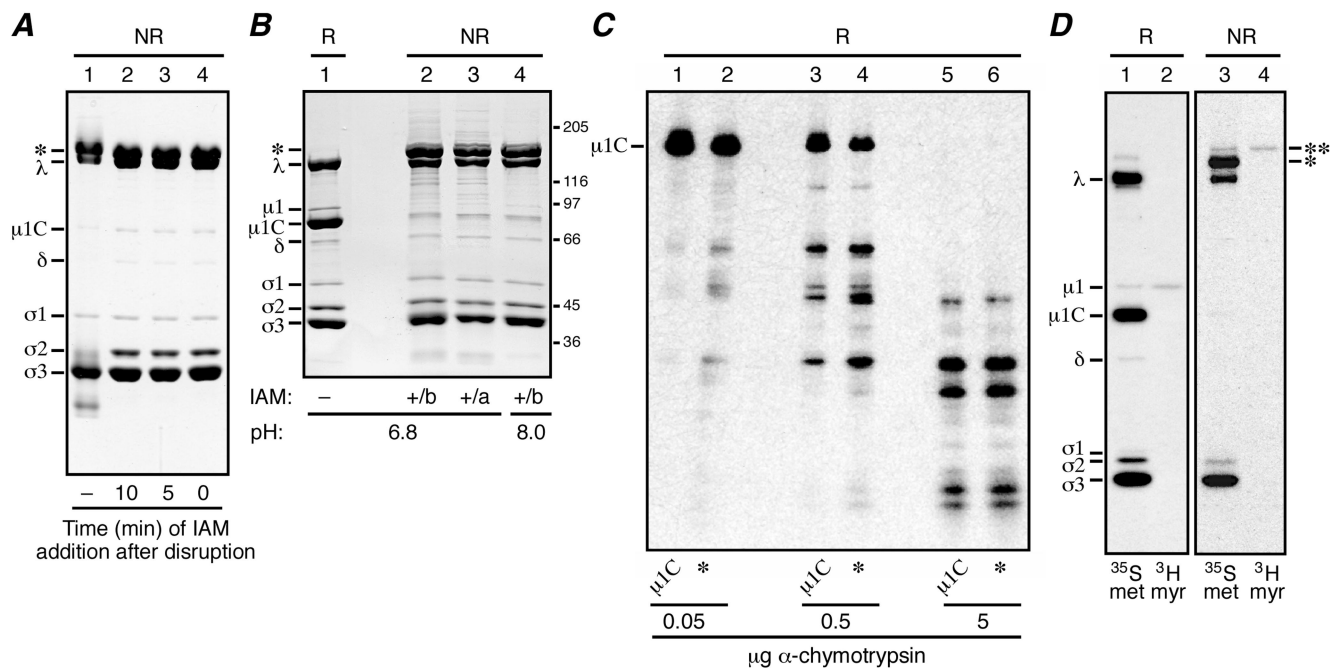


FIG. 3. Effects of IAM addition on the migration of reovirus μ 1 and μ 1C proteins during SDS-PAGE. (A and B) Purified virions of reovirus T1L were used in these experiments. Viral proteins were resolved on a mini-sized SDS-PAGE [10% (A) or 8% (B) acrylamide] gel and visualized by Coomassie staining. The major new high- M_r band observed after nonreducing disruption is indicated (*). (A) Virions were disrupted in sample buffer that contained no reducing agent (NR), and IAM was either not added (-) or added at different times after disruption (0 to 10 min) as indicated. (B) Virions were disrupted in pH 6.8 or 8.0 sample buffer that contained no reducing agent but to which 50 mM IAM was added either before (b) or immediately after (a) disruption as indicated. A sample of virions disrupted in reducing sample buffer (R; 5 mM DTT) was analyzed on the same gel (lane 1). Positions of molecular mass markers also resolved on the gel are indicated in kilodaltons. (C) Purified [35 S]methionine-cysteine-labeled virions of reovirus T3D were used in this experiment. The Coomassie-stained protein bands excised from the first gel (not shown; μ 1C was obtained from samples of reduced virions and the high- M_r band [*] was obtained from samples of IAM-treated nonreduced virions) were subjected to reduction in the gel fragments and otherwise treated as described in the text. The resulting proteins and protein fragments were resolved on a second gel and visualized by fluorography. The position of the full-length μ 1C monomer is indicated. The amount of chymotrypsin added to each gel piece atop the second gel is also indicated. (D) Purified [35 S]methionine-cysteine- or [3 H]myristate-labeled virions of reovirus T3D were mixed with reducing or nonreducing sample buffer and disrupted in a boiling water bath. The viral proteins were then resolved on a full-sized 5 to 20% acrylamide gradient SDS-PAGE gel and visualized by fluorography. The major (*) and minor (***) new high- M_r bands observed after nonreducing disruption of each sample are indicated.

ladder of minor bands that otherwise appeared in the upper half of the gel when nonreduced samples were analyzed (Fig. 3A, lane 1). IAM had these effects presumably by preventing the formation of intra- and intermolecular ds bonds in these proteins following the disruption of virions. Such bonds would be expected to form under oxidizing conditions (as in SDS-PAGE gels) once free cysteines have been exposed in the absence of a sulfhydryl-blocking agent. Use of a pH 8.0 sample buffer, instead of the standard pH 6.8 buffer (40), further decreased these other effects in the gels of nonreduced samples (Fig. 3B, lane 4), and therefore, pH 8.0 sample buffer was used in most of the later experiments. The effect of pH 8.0 probably occurs through the greater activity of IAM at this higher pH.

The small amount of uncleaved, N-terminally myristoylated μ 1 protein that appears in virions (47) (Fig. 4C, μ 1 and μ 1C) was also absent from its normal gel position when virions were disrupted under nonreducing conditions (Fig. 2 and 3). To confirm this observation, we analyzed purified T3D virions that had been metabolically labeled with [3 H]myristic acid to allow the easy identification of μ 1 (47), as shown again in this study by SDS-PAGE after disruption in reducing sample buffer (Fig. 3D, lanes 1 and 2). SDS-PAGE of the [3 H]myristate-labeled

virions after disruption in nonreducing sample buffer (50 mM IAM) showed that the radiolabel was associated with a minor new high- M_r band, which migrated slightly higher than the major new high- M_r band identified above (Fig. 3D, lanes 3 and 4). We conclude that the minor new high- M_r band represents the ds-bonded μ 1: μ 1C and/or μ 1: μ 1 dimers, while the major new high- M_r band represents ds-bonded μ 1C: μ 1C dimers.

The ϕ fragment of μ 1/ μ 1C in ISVPs is ds bonded, localizing the bond to μ 1 residue Cys679. The σ 3 and μ 1/ μ 1C proteins in reovirus virions are subject to protease cleavages during entry into host animals or cells (5, 61). σ 3 is degraded into small peptides that are released from particles, but μ 1/ μ 1C is cleaved internally to yield two stable fragments, δ and ϕ , which remain particle bound (45). The small amount of the amino-terminal, or δ , fragment of μ 1C that is commonly present in purified virions (13) appeared to migrate as a monomer after nonreducing disruption (Fig. 2 and 3). This suggested that the ds bonding of μ 1/ μ 1C may instead involve the single cysteine residue in the carboxyl (C)-terminal, or ϕ , portion of this protein (45, 66) (Fig. 4C). We treated purified T1L virions with trypsin for different times to obtain the δ - ϕ cleavage in a progressively larger proportion of μ 1/ μ 1C molecules. As the

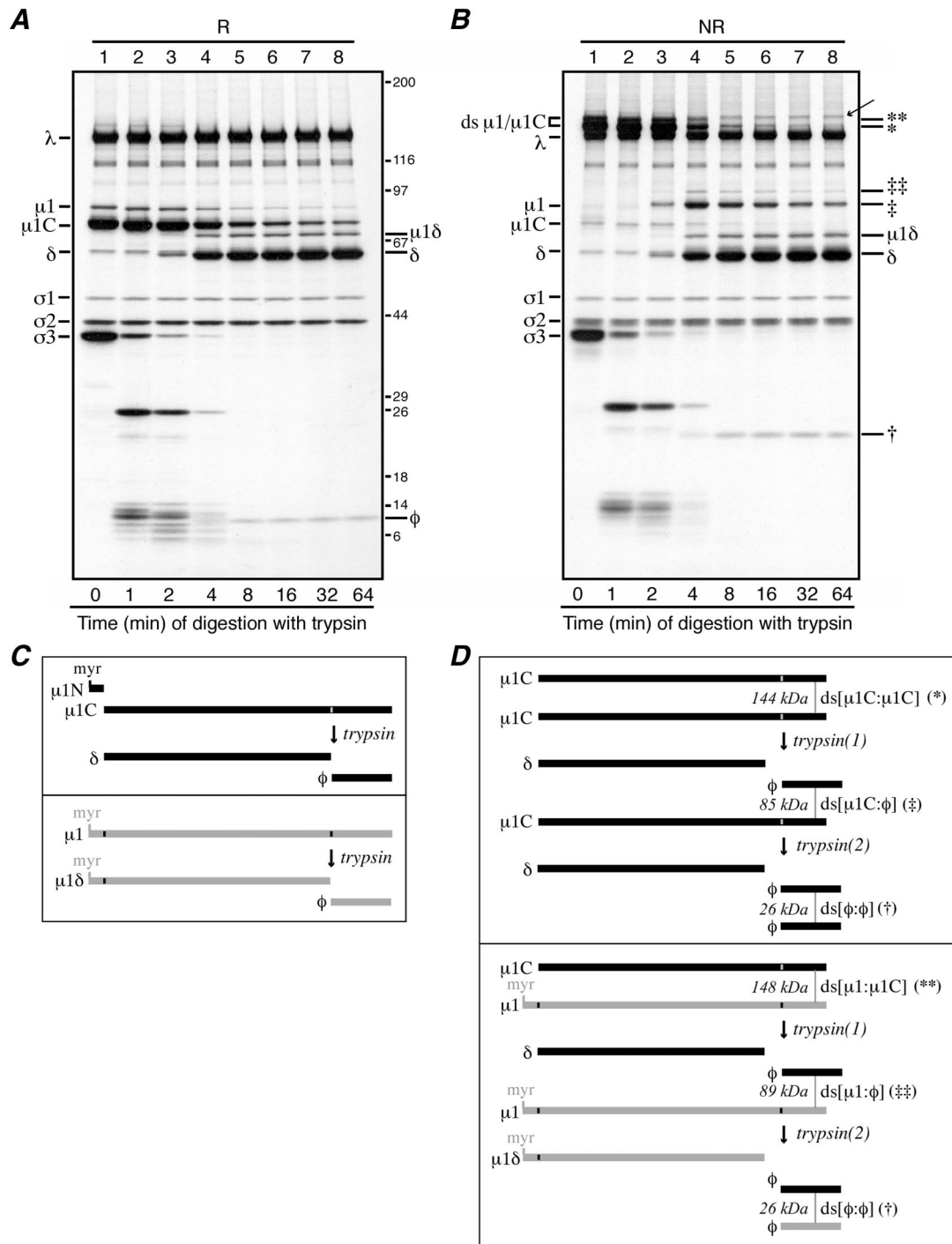


FIG. 4. Trypsin digestions of reovirus particles. (A and B) Purified [³⁵S]methionine-cysteine-labeled virions of reovirus T1L were treated with trypsin at 32°C. At each specified time, digestion was stopped by adding trypsin inhibitor. For the 0-min aliquot (lanes A1 and B1), trypsin inhibitor was added before trypsin. Each aliquot was then split in two, with half being mixed with reducing sample buffer (R) and half being mixed with nonreducing sample buffer (NR). Following disruption, proteins from the reduced (A) and nonreduced (B) samples were separately resolved on full-sized 5 to 20% acrylamide gradient SDS-PAGE gels and visualized by fluorography. The putative φ:φ homodimer band is indicated in panel B (†). The putative μ1C:φ and μ1:φ heterodimer bands are also indicated in panel B (‡ and ‡‡, respectively). A band of unknown origin in panel B, lanes 4 to 8, is indicated by an arrow; this band was not routinely observed in other experiments. Positions of molecular mass markers also resolved on the gel are indicated in kilodaltons in panel A. (C and D) The μ1 cleavage products are diagrammed, including the position of the intermolecular ds bond. Predicted molecular masses of the ds-bonded species are shown in kilodaltons. (C, upper box) Trypsin cleavage of the reduced μ1C monomer to yield monomeric fragments δ and φ. The myristoylated (myr) μ1N fragment arising along with μ1C from cleavage of full-length μ1 is also shown. (C, lower box) Trypsin cleavage of the reduced μ1 monomer to yield monomeric fragments μ1δ and φ. (D, upper box) Trypsin cleavage of the ds-bonded μ1C:μ1C homodimer. The necessity for nonsimultaneous cleavages of the two μ1C chains within each dimer results in an intermediate, heterodimer product that is later cleaved again. The first trypsin cleavage [trypsin(1)] yields a monomeric δ fragment and a ds-bonded μ1C:φ heterodimer. The second trypsin cleavage [trypsin(2)] then resolves the heterodimer into another monomeric δ fragment

$\mu 1\delta$ and δ fragments were generated, they appeared in nonreducing gels at their usual monomeric positions, with the same kinetics as and in amounts similar to those in reducing gels (Fig. 4A and B, lanes 3 to 8). The ϕ fragment was missing from its normal monomeric position in nonreducing gels (Fig. 5B), however, and a new fragment with an M_r near 25,000, or approximately twice that of ϕ , appeared with the same kinetics as and in amounts similar to those of ϕ in reducing gels (Fig. 4A, lanes 3 to 8). After reduction with BME, protein molecules from the excised 25,000- M_r band comigrated in a second SDS-PAGE gel with monomeric ϕ ($M_r \approx 12,000$) (data not shown). These results indicate that each ds bond is formed by the same residue, Cys679, from each of two $\mu 1/\mu 1C$ subunits.

The various fragments of $\mu 1$ and the likely location of the ds-bonding cysteine residue within the ϕ region are summarized in Fig. 4C and D. Monomeric $\mu 1\delta$ or δ fragments are generated in all cases, but ds-bonded $\phi:\phi$ dimers are generated only after both of the $\mu 1$ or $\mu 1C$ monomers within each original dimer are cleaved by trypsin. When the original dimers have been cleaved in only one of the constituent $\mu 1$ or $\mu 1C$ monomers, this model predicts other intermediate fragments (Fig. 4D). Bands at M_r s of 90,000 and 85,000, consistent with these predicted intermediates, $\mu 1:\phi$ and $\mu 1C:\phi$, respectively, were indeed seen in the trypsin experiments (Fig. 4B). After reduction with BME, protein molecules from the excised 85,000- M_r band comigrated in a second SDS-PAGE gel with $\mu 1C$ and ϕ (data not shown).

$\mu 1$ mutant C679S is competent for assembly but does not form ds-bonded dimers. To confirm the role of the $\mu 1$ residue Cys679 in ds bonding, we used our system for in vitro outer capsid assembly (core recoating) (8, 9). Purified cores of reovirus T1L were recoated with wt T1L $\mu 1$ and $\sigma 3$ proteins that had been expressed in insect cells from baculovirus vectors. Following purification on CsCl gradients and dialysis in virion buffer, the particles were examined by SDS-PAGE after disruption in either reducing or nonreducing sample buffer. The results demonstrated that wt T1L $\mu 1$ indeed forms ds-bonded dimers in the recoated particles (Fig. 5A, lanes 2 and 5). When a $\mu 1$ mutant containing serine in place of cysteine at position 679 (mutant C679S) was used instead, a particle band consistent with fully recoated cores was observed on the CsCl gradients (data not shown). Analysis of these particles by SDS-PAGE after disruption under reducing conditions showed that they contained similar amounts of $\mu 1/\mu 1C$ and $\sigma 3$ as virions (Fig. 5A, lane 3); after nonreducing disruption (50 mM IAM), no ds-bonded forms of $\mu 1/\mu 1C$ were seen (Fig. 5A, lane 6). These results provide further evidence that Cys679 mediates the intermolecular ds bonding of $\mu 1/\mu 1C$ and that the ds bonding is not required for assembly of the reovirus outer capsid. In addition, since the recoated cores containing C679S $\mu 1$ were successfully purified on CsCl (high-salt) gradients, these find-

ings suggest that the ds bonds are not essential for the basic stability of the outer capsid.

The $\mu 1-\sigma 3$ complexes used in the last experiment can also be purified (34) but were found to develop ds cross-links after storage at 4°C for several days in the absence of DTT (Fig. 5B, lane 4). Purified complexes containing the C679S $\mu 1$ mutant, and those containing wt $\mu 1$ treated with IAM during purification, did not (Fig. 5B, lanes 5 and 6). We concluded that Cys679 is exposed in the disordered tails of $\mu 1$, where it can be covalently modified by IAM or participate in ds bond formation between the heterohexamers in solution during storage under oxidizing conditions and at high protein concentrations. Electrospray ionization ion trap mass spectrometry of purified complexes containing wt $\mu 1$ with or without prior IAM treatment showed essentially no change in the mass of $\sigma 3$ ($\Delta = -2$ Da) but an increase in the mass of $\mu 1$ ($\Delta = 62$ Da) in the IAM-treated sample (data not shown). The latter is consistent with IAM modification of a single cysteine residue per molecule of $\mu 1$ (expected increase of 57 Da per site of modification). In contrast, purified complexes containing C679S $\mu 1$ with or without prior IAM treatment showed essentially no change in the mass of either $\sigma 3$ ($\Delta = 1$ Da) or $\mu 1$ ($\Delta = 0$ Da) (data not shown), consistent with Cys679 being the only site of IAM modification in wt $\mu 1$.

The $\mu 1/\mu 1C$ ds bonds form late in infection and are not required for virion infectivity. The dispensability of the $\mu 1/\mu 1C$ ds bonds for outer capsid assembly in vitro suggests that the ds bonds may form late in virion morphogenesis. The cytoplasm of healthy cells is strongly reducing (37, 52, 55), but late in reovirus infection, as cells are dying, the virus particles should be exposed to more oxidizing conditions (39, 63). To test this idea by varying the number of dead and dying cells that contribute virions to the purified preparations, we harvested cells at 24-h intervals postinfection and purified the cell-associated virions. IAM was added at the time of harvest to block subsequent ds bond formation. The results of this experiment revealed that the later the time of harvest, the larger the fraction of $\mu 1/\mu 1C$ that had ds bonds (Fig. 6). In fact, T1L virions harvested at 24 h postinfection contained very little ds-bonded $\mu 1/\mu 1C$ (Fig. 6, lane 1) whereas those harvested at 72 or 96 h postinfection had most of their $\mu 1/\mu 1C$ in the ds-bonded forms (Fig. 6, lanes 3 and 4). We used trypan blue to distinguish live cells from dead cells among those harvested at the different times and found a strong correlation between the percent dead cells and the percent ds-bonded $\mu 1/\mu 1C$ in the subsequently purified virions (Fig. 6). Similar results correlating cell death and $\mu 1/\mu 1C$ ds bond formation were obtained in a time course of growth and purification of T3D virions (data not shown). We concluded that ds bonding of $\mu 1/\mu 1C$ occurs in dead or dying cells in which virions are

and a ds-bonded $\phi:\phi$ homodimer. (D, lower box) Trypsin cleavage of the ds-bonded $\mu 1:\mu 1C$ heterodimer. Similar to that in panel C, the necessity for nonsimultaneous cleavages of the two chains within the dimer results in an intermediate heterodimer product that is later cleaved again. In this example, the first trypsin cleavage [trypsin(1)] acts on the $\mu 1C$ chain to yield a monomeric δ fragment and a ds-bonded $\mu 1:\phi$ heterodimer. The second trypsin cleavage [trypsin(2)] then resolves this new heterodimer into another monomeric $\mu 1\delta$ fragment and a ds-bonded $\phi:\phi$ homodimer. Not shown is the case in which the first trypsin cleavage acts on the $\mu 1$ chain in the $\mu 1:\mu 1C$ heterodimer. Also not shown is the pattern of trypsin cleavage of the $\mu 1:\mu 1$ homodimer.

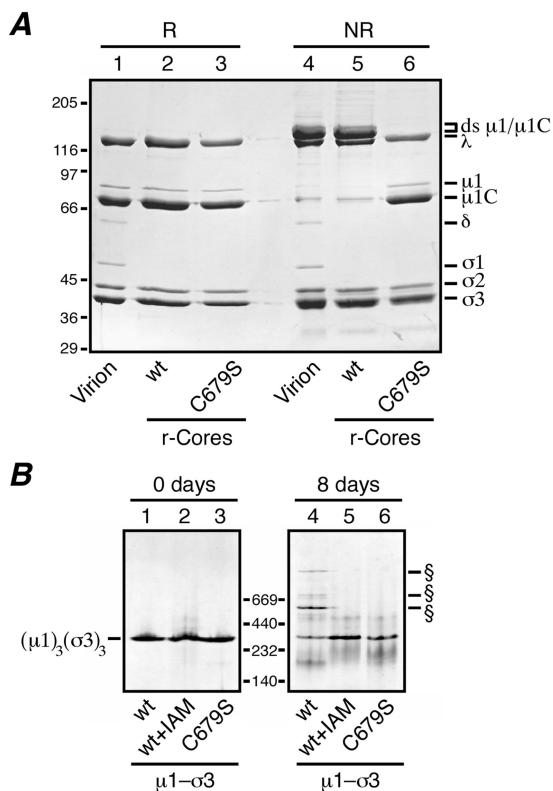


FIG. 5. Analyses for ds bond formation with $\mu 1$ mutant C679S. (A) Recoated cores containing T1L wt $\sigma 3$ and either T1L wt $\mu 1$ or the T1L $\mu 1$ mutant C679S were generated and purified, and particle concentrations were determined by densitometry. Equal amounts of the wt (lanes 2 and 5) or C679S (lanes 3 and 6) recoated cores were mixed with reducing (R) or nonreducing (NR) sample buffer, disrupted by boiling, and resolved on a mini-sized SDS-PAGE (8% acrylamide) gel. Virions disrupted under reducing (lane 1) or nonreducing (lane 4) conditions were included for comparison. Viral proteins were visualized by Coomassie staining. (B) Purified $\mu 1$ - $\sigma 3$ heterohexamers stored frozen in buffer with 10 mM DTT were thawed, and a small amount of each was diluted into nonreducing sample buffer and analyzed on a 4 to 15% acrylamide gradient native gel (Amersham Pharmacia Biotech) (lanes 1 to 3; 0 days). The remainder of each sample was passed through a PD-10 column to remove DTT and then stored at 4°C for 8 days at ambient conditions. At the end of that time, a small amount of each was diluted into sample buffer and analyzed on another 4 to 15% native gel (lanes 4 to 6). Three types of $\mu 1$ - $\sigma 3$ preparations were included in this analysis: complexes containing wt T1L $\mu 1$ and $\sigma 3$ (lanes 1 and 4), complexes containing wt T1L $\mu 1$ and $\sigma 3$ that were treated with 10 mM IAM to block free cysteines before storage (lanes 2 and 5), and complexes containing T1L C679S $\mu 1$ and wt T1L $\sigma 3$ (lanes 3 and 6). The position of the native $\mu 1$ - $\sigma 3$ heterohexamer is indicated to the left. The positions of higher- M_r forms specific to the complexes containing wt T1L $\mu 1$ and $\sigma 3$ (lanes 1) are indicated (§). Positions of native gel markers (Amersham Pharmacia Biotech) are indicated in kilodaltons.

exposed to more oxidizing conditions than are healthy cells and thus as a late step in virion morphogenesis.

The virion preparations from the preceding experiment and others like it provided sets of matched particle samples that contained differing fractions of $\mu 1/\mu 1C$ in the ds-bonded forms and could be tested for their relative, per-particle infectivity levels. In each case, these preparations showed only minor (less than twofold) differences in relative infectivity as mea-

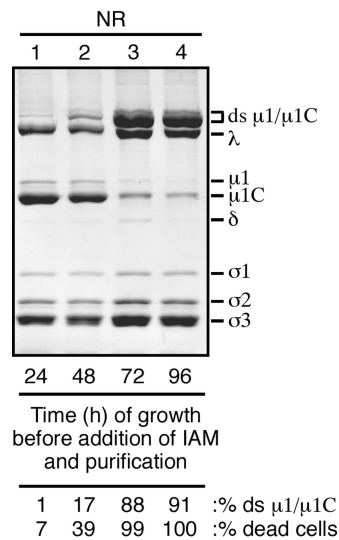


FIG. 6. Formation of the $\mu 1/\mu 1C$ ds bonds during the course of infection. T1L reovirus-infected cells were harvested at either 24, 48, 72, or 96 h postinfection. 50 mM IAM was added immediately upon resuspension of the infected cells in homogenization buffer. After purification, virions from each time point were mixed with nonreducing sample buffer (NR) and disrupted by boiling. The viral proteins were then resolved on a mini-sized SDS-8% PAGE gel. The amount of ds-bonded $\mu 1/\mu 1C$ (% ds $\mu 1/\mu 1C$) relative to the total $\mu 1$, $\mu 1C$, and ds-bonded $\mu 1/\mu 1C$ in each preparation was determined by densitometry of the Coomassie-stained gel. Immediately before harvesting, aliquots were taken from each time point and the proportion of dead/dying cells (% dead cells) was determined by trypan blue staining.

sured by plaque assays in L929 cells (data not shown). We concluded that the ds bonds are not required for the infectivity of virions in this assay system. Recoated cores containing either wt or C679S $\mu 1$ also showed essentially the same relative infectivities (data not shown), again indicating that the ds bonds are not required for infectivity.

Reversibility of the virion-associated $\mu 1/\mu 1C$ ds bonds. The preceding evidence suggested to us that the ds bonds between $\mu 1/\mu 1C$ trimers might be reversibly reduced and reformed within intact virions. We found that the $\mu 1/\mu 1C$ ds bonds in virions are indeed readily reduced over time in the presence of DTT (Fig. 7A). The virions remained intact after this treatment, as judged by their behaviors in a CsCl gradient, dialysis, and subsequent SDS-PAGE. If the newly reduced Cys679 residues were blocked with IAM before reisolation on the CsCl gradient, the particles displayed $\mu 1/\mu 1C$ almost exclusively as monomers on the gel (data not shown). If the newly reduced Cys679 residues were not blocked with IAM before reisolation on the gradient, however, the particles displayed $\mu 1/\mu 1C$ almost exclusively as dimers on the gel (data not shown), indicating that the ds bonds had efficiently reformed in the gradient and/or dialysis. To reform the ds bonds in virions in a more controlled manner, we first reduced them with DTT and then removed the DTT by dialysis and used SDS-PAGE to monitor their reformation over time. If no additional reagent was added, the ds bonds reformed very slowly, if at all (Fig. 7B, lane 9). If cystine (cysteine ds; 5 mM) was added to promote ds exchange, however, the bonds reformed rapidly and to near completion over a 3-h time course (Fig. 7B, lanes 1 to 8). The

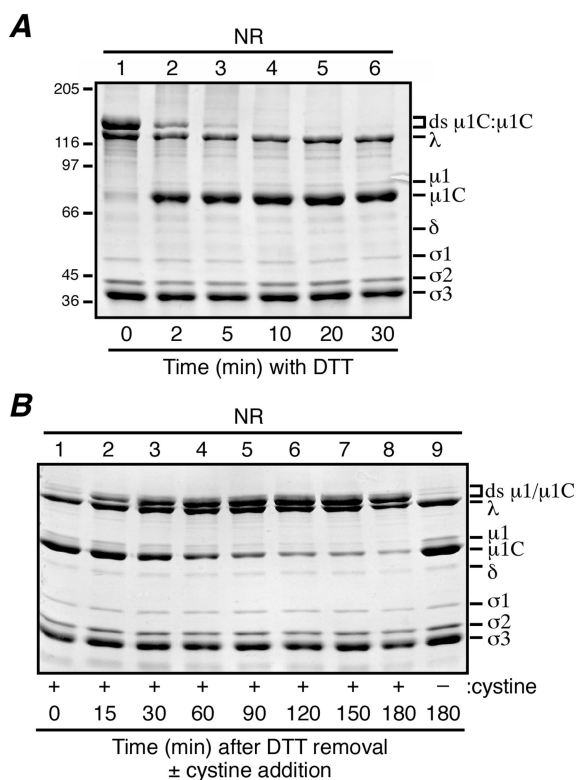


FIG. 7. Reversibility of the virion-associated $\mu 1 / \mu 1 C$ ds bonds. For each experiment, aliquots were removed from the reaction mixture at the indicated intervals, and the reaction was quenched with 50 mM IAM. When all samples had been collected for each experiment, they were mixed with nonreducing sample buffer (NR) and disrupted by boiling. Viral proteins were resolved on mini-sized SDS-8% PAGE gels and visualized by Coomassie staining. (A) DTT at a concentration of 5 mM was added to purified T1L virions and allowed to incubate at room temperature to effect in situ reduction of the ds bonds. The 0-min aliquot (lane 1) was removed before the addition of DTT. Positions of molecular mass markers also resolved on the gel are indicated to the left. (B) The ds bonds in a sample of T1L virions were reduced by DTT as in panel A, lane 6, after which the DTT was removed by dialysis. Cystine at a concentration of 5 mM was then added to promote in situ reformation of the ds bonds. The 0-min aliquot (lane 1) was removed before the addition of cystine. A sample to which cysteine was never added was also analyzed (lane 9).

virions remained intact after this treatment as well (data not shown). These findings indicate that the positions of the 600 $\mu 1$ Cys679 residues within the virion outer capsid allow them to form intermolecular ds bonds that can be reversibly broken and reforged with high efficiency and without substantially affecting the other structural features of the particle.

DISCUSSION

Where are the $\mu 1 / \mu 1 C$ ds bonds located in the reovirus outer capsid? The 33 C-terminal residues of $\mu 1$ beyond Pro675 are disordered in the crystallized $\mu 1$ - $\sigma 3$ heterohexamers (34) and are thus likely to be solvent exposed. The crystallographic model of the heterohexamer fits well into an 18-Å resolution density map of the reovirus virion obtained by cryoEM, indicating that only limited rearrangements in the heterohexamers must take place in building the outer capsid (34). In the fitted

model, Pro675 is on an exposed surface of $\mu 1$ about one-third of the distance from the base to the top of the complex and faces into the solvent channels that are surrounded by $\mu 1$ trimers in the fenestrated $T=13$ lattice (16, 42) (Fig. 1 and 8). Cys679 must lie within about 15 Å (four extended peptide bonds) of Pro675, strongly suggesting that the ds bonds are formed within the channels where the C-proximal portions of the surrounding $\mu 1$ subunits approach each other (Fig. 8). This arrangement determines that the ds bonds are formed between subunits from adjacent trimers; they cannot form between subunits from the same trimer because Cys679 from each projects into a different channel (34) (Fig. 8).

A blob of density observed in each P3 channel in cryoEM reconstructions of virions (15, 16) (Fig. 1 and 8) can be attributed to a clustering of the 33-residue C-terminal tails of the six surrounding $\mu 1$ subunits (34). We previously suggested that these six C-terminal tails interact to form a small globular domain, perhaps resembling the β annulus at the local sixfold positions in some plant RNA viruses (34). A substantially higher-resolution map of reovirus virions recently obtained by cryoEM and 3D reconstruction is consistent with this suggestion (X. Zhang, S. B. Walker, M. L. Nibert, and T. S. Baker, unpublished data). The higher-resolution map also suggests that a similar small domain can be found within each P2 channel (Fig. 1 and 8), although formed by the C-terminal tails of only the four $\mu 1$ subunits that surround each of those channels. The precise placements of the ds bonds within these channel-associated structures, and the role of the ds bonds in assembling them, remain to be determined.

Nearly all (>90%) of the $\mu 1 / \mu 1 C$ subunits in virions participate in ds bonds (Fig. 6 and 7). Thus, within the channels, there must be pairwise linkage of the six (P3) or four (P2) adjacent $\mu 1$ arms. ds exchange between neighboring cysteine/cystine residues is likely to guarantee that few, if any, free cysteines remain around either type of channel once ds bond formation is complete (Fig. 8). The ds bonds thereby create a network of intertrimer cross-links that span the whole outer capsid, except for the regions of fenestration around the five-fold axes where $\lambda 2$ is found (Fig. 8). This aspect of the reovirus $\mu 1$ -associated ds bonds is reminiscent of the interpentamer ds bonds of the papovavirus capsid proteins and could have similar consequences for assembly and disassembly (22, 31, 33, 53). Our data argue against a required role for the ds bonds in reovirus assembly, however.

When and how are the $\mu 1 / \mu 1 C$ ds bonds formed during infection? Evidence that the $\mu 1 / \mu 1 C$ ds bonds form as a late step in virion morphogenesis, temporally correlated with cell death, suggests these bonds may not be formed until cell health is compromised, exposing the assembled virions to a more oxidizing environment. In healthy cells, a reducing environment is maintained through the generation of large amounts of NADPH and the subsequent maintenance of the reduced forms of flavin adenine dinucleotide, glutathione, and various ds reductases such as thio- and glutaredoxins (52, 55). It is unusual for ds bonds in intracellular proteins to survive for long in this environment (1, 26, 37, 52, 55). Oxidative stress, with resulting drops in the cellular levels of antioxidants, is associated with both apoptotic and necrotic cell death (39, 49) and would be expected to promote ds bond formation in both cellular and viral proteins. Formation of the intermolecular ds

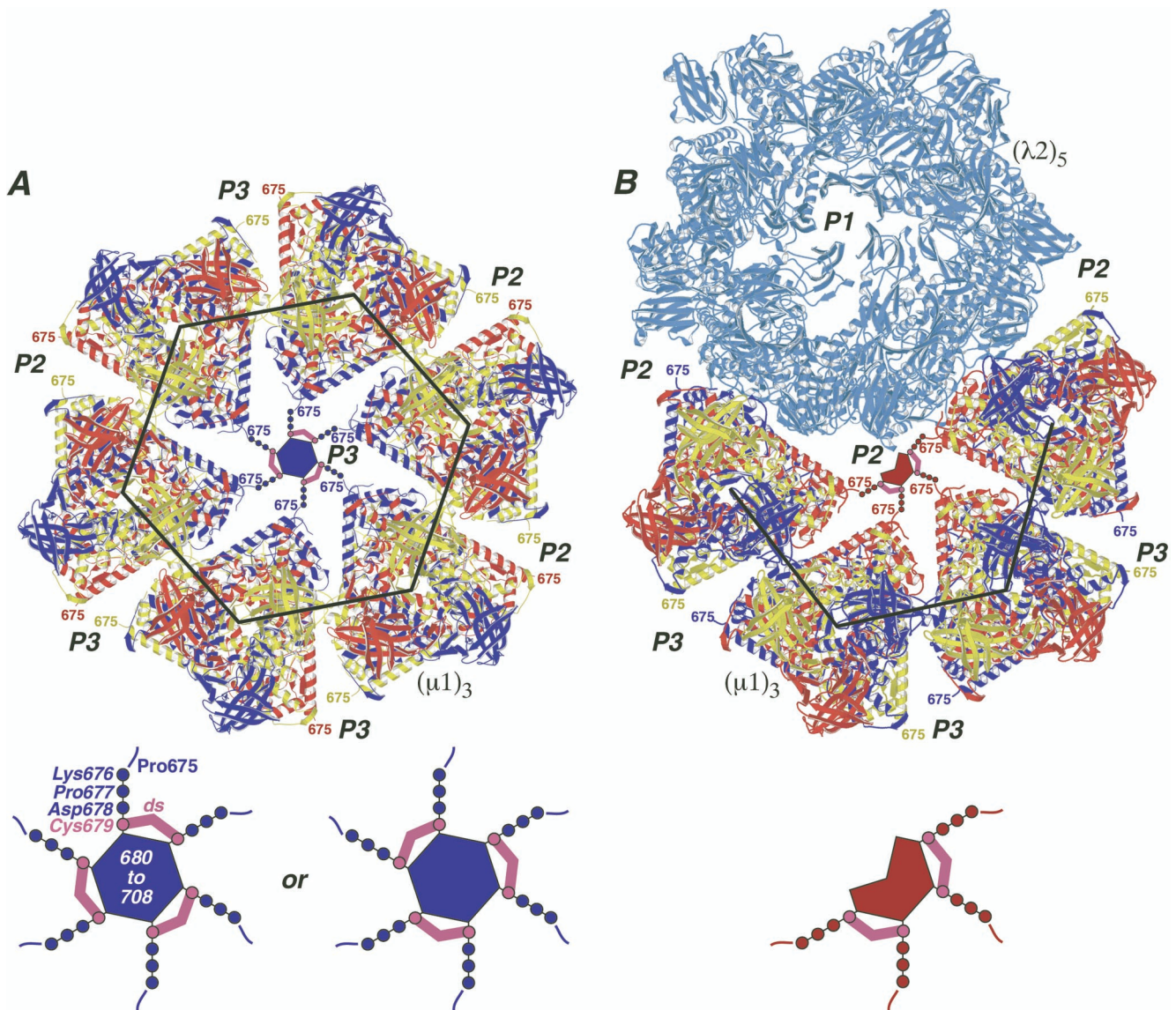


FIG. 8. Locations of the ds bonds in the $\mu 1$ outer capsid structure. The crystal structure of $\mu 1$ was extracted from the $\mu 1$ - $\sigma 3$ heterohexameric complex and positioned as it appears on the surface of the virion (34). Each $\mu 1$ trimer [$(\mu 1)_3$] is colored blue, red, and yellow to represent the three individual $\mu 1$ subunits. The large black hexagon and partial hexagon indicate the respectively marked regions in Fig. 1 except that the $\sigma 3$ subunits are missing and the region of the partial hexagon is rotated downward by approximately 60° relative to that in Fig. 1. (A) Six $\mu 1$ trimers are shown surrounding one of the 60 P3 channels. Surrounding channels are also labeled (P2 or P3). The C-terminal residue in the $\mu 1$ crystal structure, Pro675, faces into the channels and is labeled in each of the $\mu 1$ subunits. A model for $\mu 1$ residues 676 to 708, which were not visualized in the crystal structure of the $\mu 1$ - $\sigma 3$ heterohexameric complex (34), is shown within the P3 channel that is central in this image. Cys679 and its ds bonds are shown in magenta. Residues 676 to 678 and 680 to 708 are shown in blue to match the six surrounding $\mu 1$ subunits from which they extend. Residues 680 to 708 are proposed to form the central blob evident in Fig. 1 and discussed in the text and reference 34. A magnified view of these modeled features is shown at the bottom, with labels for residues 675 to 708 and a ds bond. The alternative arrangement of the three ds bonds is shown at bottom right. (B) Four $\mu 1$ trimers and a $\lambda 2$ pentamer [$(\lambda 2)_5$] (light blue) are shown surrounding one of the 60 P2 solvent channels. The P1 channel, which is surrounded by the five $\lambda 2$ subunits and plugged by $\sigma 1$ in virions (not shown), is included and labeled in this view. A model for $\mu 1$ residues 676 to 708 is shown within the P2 channel that is central in this image. Other labeling and color coding is as described for panel A, except that residues 676 to 678 and 680 to 708 are shown in red to match the four surrounding $\mu 1$ subunits from which they extend.

bonds in $\mu 1/\mu 1C$ may thus be a marker for changes in the intracellular redox potential associated with reovirus-induced cell injury or death (63).

Whether formation of the $\mu 1/\mu 1C$ ds bonds is inherent to virion-associated $\mu 1$ or requires direct input from another viral or cellular factor remains to be determined. It is notable, however, that the reduced ds bonds reformed only slowly, if at

all, at ambient *in vitro* redox conditions (Fig. 7B, lane 9) but very rapidly once cystine molecules capable of ds exchange were added (Fig. 7B, lanes 1 to 8). We speculate that the conditions in dead or dying cells, with high concentrations of ds-exchanging prooxidants such as glutathione ds (39), may promote the efficient formation of these bonds. We therefore propose that the stable ds bonds in reovirus virions form pri-

marily within such cells rather than after their release into the extracellular environment. This hypothesis may be relevant to the formation of similar ds bonds in the capsids of other non-enveloped viruses as well.

What roles might the μ 1/ μ 1C ds bonds play in reovirus infection and biology? Cys679 is conserved in all the reovirus isolates for which the encoding M2 gene sequence has been determined to date: not only T1L and T3D (24, 66) but also type 2 Jones (66), type 3 Abney (20), and type 3 clone 8 (25). Although this list comprises a limited number of strains, the conservation of Cys679 is consistent with its ds bonds granting an advantage at some step in infection. Cys679 was not conserved, however, in three recently determined homologous sequences from related viruses: two M2/ μ B sequences from avian reoviruses (R. Duncan, personal communication) and three M6/VP4 sequences from aquareoviruses (2, 50). This variation suggests an evolutionary or host range difference in the role of the ds bonds.

One possible, though perhaps unlikely, role for the μ 1/ μ 1C ds bonds is as a thiol oxidoreductase for one or more cellular or viral substrates. If this substrate were involved in redox sensing and signaling (1), then the μ 1/ μ 1C ds bonds could influence cell health or metabolism. Although these ds bonds do not form stably until late in infection, it is possible that they are formed more transiently (reversibly formed and broken) earlier on. Thus, they could have an effect on cells well before cell death. We have shown in two different ways (C679S mutant and time course of purification) that the ds bonds are not required for virion assembly. In fact, the locations of the ds bonds in the P2 and P3 channels make it easy to see how they can form within the fully assembled outer capsid. Neither are these bonds needed for the basic stability of virions, since virions lacking or containing very few of them can be subjected to the standard purification protocol and yet remain structurally intact and fully infectious. It remains possible, nonetheless, that the ds bonds may enhance the stability of reovirus virions under certain conditions, such as those encountered outside host animals or during entry through the gastrointestinal tracts of those hosts. A clear direction for future work is to define the roles of these bonds and the advantage(s) they may grant to mammalian reoviruses.

The possible effects of the μ 1/ μ 1C ds bonds on reovirus entry are interesting to consider. Given these bonds are not required for infectivity, one can imagine they may in fact impede membrane penetration by restricting the conformational freedom of μ 1 (7, 20). Moreover, if μ 1 release from particles is an obligatory step during entry (7, 14, 20), then reduction of the ds bonds may be necessary to resolve the capsid-wide cross-linking of the μ 1 trimers that the ds bonds bestow. The ease with which the ds bonds can be reduced in intact virions (Fig. 7A) suggests that the bonds may indeed be severed during the entry of infecting reovirus particles, and our preliminary evidence suggests this is the case.

ACKNOWLEDGMENTS

We are grateful to David King at the Howard Hughes Medical Institute, University of California at Berkeley, for performing mass spectrometry analyses and providing the description of his methods; Laura Breun and Elaine Freimont for excellent technical support; and the other members of our laboratories for helpful discussions. We also thank Timothy Baker and Jonathan Beckwith for reviewing a draft of

the manuscript and Timothy Baker, Roy Duncan, and Xing Zhang for sharing information before publication.

This work was partially supported by NIH grants R01 AI-46440 (to M.L.N.) and R01 CA-13202 (to S.C.H.). K.C. was supported by a predoctoral fellowship from the Howard Hughes Medical Institute and by a Fields Postdoctoral Fellowship from the Department of Microbiology and Molecular Genetics. S.L. was supported by a postdoctoral BASF research fellowship of the Studienstiftung des Deutschen Volkes and as an associate of the Howard Hughes Medical Institute. S.C.H. is an investigator at the Howard Hughes Medical Institute.

REFERENCES

1. Aslund, F., and J. Beckwith. 1999. Bridge over troubled waters: sensing stress by disulfide bond formation. *Cell* **96**:751–753.
2. Attoui, H., Q. Fang, F. M. Jaafar, J. F. Cantaloube, P. Biagini, P. De Micco, and X. De Lamballerie. 2002. Common evolutionary origin of aquareoviruses and orthoreoviruses revealed by genome characterization of Golden shiner reovirus, Grass carp reovirus, Striped bass reovirus and golden ide reovirus (genus Aquareovirus, family Reoviridae). *J. Gen. Virol.* **83**:1941–1951.
3. Barton, E. S., J. L. Connolly, J. C. Forrest, J. D. Chappell, and T. S. Dermody. 2000. Utilization of sialic acid as a coreceptor enhances reovirus attachment by multi-step adhesion-strengthening. *J. Biol. Chem.* **276**:2200–2211.
4. Barton, E. S., J. C. Forrest, J. L. Connolly, J. D. Chappell, Y. Liu, F. J. Schnell, A. Nusrat, C. A. Parkos, and T. S. Dermody. 2001. Junction adhesion molecule is a receptor for reovirus. *Cell* **104**:441–451.
5. Bodkin, D. K., M. L. Nibert, and B. N. Fields. 1989. Proteolytic digestion of reovirus in the intestinal lumens of neonatal mice. *J. Virol.* **63**:4676–4681.
6. Braakman, I., H. Hoover-Litty, K. R. Wagner, and A. Helenius. 1991. Folding of influenza hemagglutinin in the endoplasmic reticulum. *J. Cell Biol.* **114**:401–411.
7. Chandran, K., D. L. Farsetta, and M. L. Nibert. 2002. Strategy for nonenveloped virus entry: a hydrophobic conformer of the reovirus membrane penetration protein μ 1 mediates membrane disruption. *J. Virol.* **76**:9920–9933.
8. Chandran, K., S. B. Walker, Y. Chen, C. M. Contreras, L. A. Schiff, T. S. Baker, and M. L. Nibert. 1999. In vitro recoding of reovirus cores with baculovirus-expressed outer-capsid proteins μ 1 and σ 3. *J. Virol.* **73**:3941–3950.
9. Chandran, K., X. Zhang, N. O. Olson, S. B. Walker, J. D. Chappell, T. S. Dermody, T. S. Baker, and M. L. Nibert. 2001. Complete in vitro assembly of the reovirus outer capsid produces highly infectious particles suitable for genetic studies of the receptor-binding protein. *J. Virol.* **75**:5335–5342.
10. Chappell, J. D., A. E. Porta, T. S. Dermody, and T. Stehle. 2002. Crystal structure of reovirus attachment protein σ 1 reveals evolutionary relationship to adenovirus fiber. *EMBO J.* **21**:1–11.
11. Cleveland, D. R., H. Zarbl, and S. Millward. 1986. Reovirus guanylyltransferase is L2 gene product lambda 2. *J. Virol.* **60**:307–311.
12. Cleveland, D. W. 1983. Peptide mapping in one dimension by limited proteolysis of sodium dodecyl sulfate-solubilized proteins. *Methods Enzymol.* **96**:222–229.
13. Coombs, K. M. 1998. Stoichiometry of reovirus structural proteins in virus, ISVP, and core particles. *Virology* **243**:218–228.
14. Drayna, D., and B. N. Fields. 1982. Activation and characterization of the reovirus transcriptase: genetic analysis. *J. Virol.* **41**:110–118.
15. Dryden, K. A., D. L. Farsetta, G. Wang, J. M. Keegan, B. N. Fields, T. S. Baker, and M. L. Nibert. 1998. Internal structures containing transcriptase-related proteins in top component particles of mammalian orthoreovirus. *Virology* **245**:33–46.
16. Dryden, K. A., G. Wang, M. Yeager, M. L. Nibert, K. M. Coombs, D. B. Furlong, B. N. Fields, and T. S. Baker. 1993. Early steps in reovirus infection are associated with dramatic changes in supramolecular structure and protein conformation: analysis of virions and subviral particles by cryoelectron microscopy and image reconstruction. *J. Cell Biol.* **122**:1023–1041.
17. Fausnaugh, J., and A. J. Shatkin. 1990. Active site localization in a viral mRNA capping enzyme. *J. Biol. Chem.* **265**:7669–7672.
18. Furlong, D. B., M. L. Nibert, and B. N. Fields. 1988. Sigma 1 protein of mammalian reoviruses extends from the surfaces of viral particles. *J. Virol.* **62**:246–256.
19. Hazelton, P. R., and K. M. Coombs. 1995. The reovirus mutant tsA279 has temperature-sensitive lesions in the M2 and L2 genes: the M2 gene is associated with decreased viral protein production and blockade in transmembrane transport. *Virology* **207**:46–58.
20. Hooper, J. W., and B. N. Fields. 1996. Role of the μ 1 protein in reovirus stability and capacity to cause chromium release from host cells. *J. Virol.* **70**:459–467.
21. Huismans, H., and W. K. Joklik. 1976. Reovirus-coded polypeptides in infected cells: isolation of two native monomeric polypeptides with affinity for single-stranded and double-stranded RNA, respectively. *Virology* **70**:411–424.

22. **Ishizu, K. I., H. Watanabe, S. I. Han, S. N. Kanesashi, M. Hoque, H. Yajima, K. Kataoka, and H. Handa.** 2001. Roles of disulfide linkage and calcium ion-mediated interactions in assembly and disassembly of virus-like particles composed of simian virus 40 VP1 capsid protein. *J. Virol.* **75**:61–72.
23. **Jané-Valbuena, J., M. L. Nibert, S. M. Spencer, S. B. Walker, T. S. Baker, Y. Chen, V. E. Centonze, and L. A. Schiff.** 1999. Reovirus virion-like particles obtained by recoating infectious subvirion particles with baculovirus-expressed $\sigma 3$ protein: an approach for analyzing $\sigma 3$ functions during virus entry. *J. Virol.* **73**:2963–2973.
24. **Jayasuriya, A. K., M. L. Nibert, and B. N. Fields.** 1988. Complete nucleotide sequence of the M2 gene segment of reovirus type 3 dearing and analysis of its protein product $\mu 1$. *Virology* **163**:591–602.
25. **Jayasuriya, A. K. A.** 1991. Ph.D. thesis. Harvard University, Cambridge, Mass.
26. **Kadokura, H., and J. Beckwith.** 2001. The expanding world of oxidative protein folding. *Nat. Cell Biol.* **3**:E247–E249.
27. **Kraulis, P. J.** 1991. MOLSCRIPT: a program to produce both detailed and schematic plots of protein structures. *J. Appl. Crystallogr.* **24**:946–950.
28. **Krishnaswamy, S., and M. G. Rossmann.** 1990. Structural refinement and analysis of Mengo virus. *J. Mol. Biol.* **211**:803–844.
29. **Laemmlis, U. K.** 1970. Cleavage of structural proteins during the assembly of the head of bacteriophage T4. *Nature* **227**:680–685.
30. **Lee, P. W. K., E. C. Hayes, and W. K. Joklik.** 1981. Protein $\sigma 1$ is the reovirus cell attachment protein. *Virology* **108**:156–163.
31. **Li, M., P. Beard, P. A. Estes, M. K. Lyon, and R. L. Garcea.** 1998. Intercapsomeric disulfide bonds in papillomavirus assembly and disassembly. *J. Virol.* **72**:2160–2167.
32. **Li, P. P., A. Nakanishi, S. W. Clark, and H. Kasamatsu.** 2002. Formation of transitory intrachain and interchain disulfide bonds accompanies the folding and oligomerization of simian virus 40 Vp1 in the cytoplasm. *Proc. Natl. Acad. Sci. USA* **99**:1353–1358.
33. **Li, P. P., A. Nakanishi, M. A. Tran, A. M. Salazar, R. C. Liddington, and H. Kasamatsu.** 2000. Role of simian virus 40 Vp1 cysteines in virion infectivity. *J. Virol.* **74**:11388–11393.
34. **Liemann, S., K. Chandran, T. S. Baker, M. L. Nibert, and S. C. Harrison.** 2002. Structure of the reovirus membrane-penetration protein, $\mu 1$, in a complex with its protector protein, $\sigma 3$. *Cell* **108**:283–295.
35. **Logan, D., R. Abu-Ghazaleh, W. Blakemore, S. Curry, T. Jackson, A. King, S. Lea, R. Lewis, J. Newman, N. Parry, et al.** 1993. Structure of a major immunogenic site on foot-and-mouth disease virus. *Nature* **362**:566–568.
36. **Lucia-Jandris, P., J. W. Hooper, and B. N. Fields.** 1993. Reovirus M2 gene is associated with chromium release from mouse L cells. *J. Virol.* **67**:5339–5345.
37. **Mallick, P., D. R. Boutz, D. Eisenberg, and T. O. Yeates.** 2002. Genomic evidence that the intracellular proteins of archaeal microbes contain disulfide bonds. *Proc. Natl. Acad. Sci. USA* **99**:9679–9684.
38. **Mao, Z. X., and W. K. Joklik.** 1991. Isolation and enzymatic characterization of protein $\lambda 2$, the reovirus guanylyltransferase. *Virology* **185**:377–386.
39. **Martin, L. J.** 2001. Neuronal cell death in nervous system development, disease, and injury. *Int. J. Mol. Med.* **7**:455–478.
40. **McGrath, W. J., K. S. Aherne, and W. F. Mangel.** 2002. In the virion, the 11-amino-acid peptide cofactor pVIc is covalently linked to the adenovirus proteinase. *Virology* **296**:234–240.
41. **Merritt, E. A., and M. E. P. Murphy.** 1994. Raster 3D version 2.0. A program for photorealistic molecular graphics. *Acta Crystallogr. Sect. D. Biol. Crystallogr.* **50**:869–873.
42. **Metcalf, P., M. Cyrklaff, and M. Adrian.** 1991. The three-dimensional structure of reovirus obtained by cryo-electron microscopy. *EMBO J.* **10**:3129–3136.
43. **Middleton, J. K., T. F. Severson, K. Chandran, A. L. Gillian, J. Yin, and M. L. Nibert.** 2002. Thermostability of reovirus disassembly intermediates (ISVPs) correlates with genetic, biochemical, and thermodynamic properties of major surface protein $\mu 1$. *J. Virol.* **76**:1051–1061.
44. **Mirazimi, A., and L. Svensson.** 2000. ATP is required for correct folding and disulfide bond formation of rotavirus VP7. *J. Virol.* **74**:8048–8052.
45. **Nibert, M. L., and B. N. Fields.** 1992. A carboxy-terminal fragment of protein $\mu 1/\mu 1C$ is present in infectious subvirion particles of mammalian reoviruses and is proposed to have a role in penetration. *J. Virol.* **66**:6408–6418.
46. **Nibert, M. L., and L. A. Schiff.** 2001. Reoviruses and their replication, p. 1679–1728. *In* D. M. Knipe and P. M. Howley (ed.), *Fields virology*, 4th ed. Lippincott Williams & Wilkins, Philadelphia, Pa.
47. **Nibert, M. L., L. A. Schiff, and B. N. Fields.** 1991. Mammalian reoviruses contain a myristoylated structural protein. *J. Virol.* **65**:1960–1967.
48. **Patton, J. T., J. Hua, and E. A. Mansell.** 1993. Location of intrachain disulfide bonds in the VP5* and VP8* trypsin cleavage fragments of the rhesus rotavirus spike protein VP4. *J. Virol.* **67**:4848–4855.
49. **Pias, E. K., and T. Y. Aw.** 2002. Apoptosis in mitotic competent undifferentiated cells is induced by cellular redox imbalance independent of reactive oxygen species production. *FASEB J.* **16**:781–790.
50. **Qiu, T., R. H. Lu, J. Zhang, and Z. Y. Zhu.** 2001. Molecular characterization and expression of the M6 gene of grass carp hemorrhage virus (GCHV), an aquareovirus. *Arch. Virol.* **146**:1391–1397.
51. **Reinisch, K. M., M. L. Nibert, and S. C. Harrison.** 2000. Structure of the reovirus core at 3.6 Å resolution. *Nature* **404**:960–967.
52. **Rietsch, A., and J. Beckwith.** 1998. The genetics of disulfide bond metabolism. *Annu. Rev. Genet.* **32**:163–184.
53. **Schmidt, U., R. Rudolph, and G. Bohm.** 2000. Mechanism of assembly of recombinant murine polyomavirus-like particles. *J. Virol.* **74**:1658–1662.
54. **Segal, M. S., J. M. Bye, J. F. Sambrook, and M. J. Gething.** 1992. Disulfide bond formation during the folding of influenza virus hemagglutinin. *J. Cell Biol.* **118**:227–244.
55. **Senkevich, T. G., C. L. White, E. V. Koonin, and B. Moss.** 2002. Complete pathway for protein disulfide bond formation encoded by poxviruses. *Proc. Natl. Acad. Sci. USA* **99**:6667–6672.
56. **Senkevich, T. G., C. L. White, E. V. Koonin, and B. Moss.** 2000. A viral member of the ERV1/ALR protein family participates in a cytoplasmic pathway of disulfide bond formation. *Proc. Natl. Acad. Sci. USA* **97**:12068–12073.
57. **Shing, M., and K. M. Coombs.** 1996. Assembly of the reovirus outer capsid requires $\mu 1/\sigma 3$ interactions which are prevented by misfolded $\sigma 3$ protein in temperature-sensitive mutant tsG453. *Virus Res.* **46**:19–29.
58. **Smith, R. E., H. J. Zweerink, and W. K. Joklik.** 1969. Polypeptide components of virions, top component and cores of reovirus type 3. *Virology* **39**:791–810.
59. **Spencer, S. M., J. Y. Sgro, K. A. Dryden, T. S. Baker, and M. L. Nibert.** 1997. IRIS explorer software for radial-depth cueing reovirus particles and other macromolecular structures determined by cryoelectron microscopy and image reconstruction. *J. Struct. Biol.* **120**:11–21.
60. **Strong, J. E., G. Leone, R. Duncan, R. K. Sharma, and P. W. K. Lee.** 1991. Biochemical and biophysical characterization of the reovirus cell attachment protein $\sigma 1$: evidence that it is a homotrimer. *Virology* **184**:23–32.
61. **Sturzenbecker, L. J., M. Nibert, D. Furlong, and B. N. Fields.** 1987. Intracellular digestion of reovirus particles requires a low pH and is an essential step in the viral infectious cycle. *J. Virol.* **61**:2351–2361.
62. **Tijssen, P., and E. Kurstak.** 1981. Biochemical, biophysical, and biological properties of densovirus (parvovirus). III. Common sequences of structural proteins. *J. Virol.* **37**:17–23.
63. **Tyler, K. L., P. Clarke, R. L. DeBiasi, D. Kominsky, and G. J. Poggioli.** 2001. Reoviruses and the host cell. *Trends Microbiol.* **9**:560–564.
64. **White, C. K., and H. J. Zweerink.** 1976. Studies on the structure of reovirus cores: selective removal of polypeptide $\lambda 2$. *Virology* **70**:171–180.
65. **White, C. L., T. G. Senkevich, and B. Moss.** 2002. Vaccinia virus G4L glutaredoxin is an essential intermediate of a cytoplasmic disulfide bond pathway required for virion assembly. *J. Virol.* **76**:467–472.
66. **Wiener, J. R., and W. K. Joklik.** 1988. Evolution of reovirus genes: a comparison of serotype 1, 2, and 3 M2 genome segments, which encode the major structural capsid protein $\mu 1C$. *Virology* **163**:603–613.